Improved dynamic equations for the generally configured Stewart platform manipulator [†]

Siamak Pedrammehr[1,*], Mehran Mahboubkhah[1] and Navid Khani[2]

[1]*Faculty of Mechanical Engineering, University of Tabriz, Bahman 29th Blvd., 51666-14766, Tabriz, Iran*
[2]*School of Mechanical Engineering, College of Engineering, University of Tehran, 14395-515, Tehran, Iran*

Abstract

In this paper, a Newton-Euler approach is utilized to generate the improved dynamic equations of the generally configured Stewart platform. Using the kinematic model of the universal joint, the rotational degree of freedom of the pods around the axial direction is taken into account in the formulation. The justifiable direction of the reaction moment on each pod is specified and considered in deriving the dynamic equations. Considering the theorem of parallel axes, the inertia tensors for different elements of the manipulator are obtained in this study. From a theoretical point, the improved formulation is more accurate in comparison with previous ones, and the necessity of the improvement is clear evident from significant differences in the simulation results for the improved model and the model without improvement. In addition to more feasibility of the structure and higher accuracy, the model is highly compatible with computer arithmetic and suitable for online applications for loop control problems in hardware.

Keywords: Dynamic equations; Newton-Euler approach; Stewart platform

---

1. Introduction

Closed-loop structures and kinematic constraints make it especially difficult to solve the kinematic and dynamics of a parallel manipulator such as Stewart platform [1]. As the manipulator real-time control is necessary, computation of the manipulator dynamics should be highly accurate.

In the literature of the kinematics and dynamics of the parallel manipulation, several approaches have been used according to the classical mechanics principles such as: the principle of virtual work [2-5], Kane's method [6, 7] momentum approach [8, 9], Hamilton's principle [10], screw theory [11] and recursive matrix method [12]. Furthermore, the Euler-Lagrange and the Newton-Euler methods are the most popular approaches which are applied to the dynamic analysis of Stewart platform [9]. The Euler-Lagrange method imposes the kinematic constraints by Lagrange multipliers and leads to a system of differential equation which is too complicated to solve. The Lagrangian approach has been developed by Geng et al. [13] to solve the inverse dynamics of the Stewart platform. Lebret et al. [14] also utilized same method to derive the motion equation of Stewart platform. Ting et al. [15] used the

Euler-Lagrange method to derive a complete dynamic model of Gough-Stewart platform-type computer numerical control (CNC) machine. The rotation terms of the pods are considered in their study and it is shown that these terms cannot be neglected in the machine tool applications. Wang et al. [16] employed the Lagrange formulation to solve the dynamics of the hydraulic Stewart platform, considering the effect of pod inertia. Guo and Li [17] combined the Lagrange formulation with the Newton-Euler method for deriving the compact closed-form dynamic equations of the Stewart platform manipulator. In Newton-Euler method, Newton's law and Euler's equation are applied to rigid bodies. This method is efficient enough for the inverse dynamics solution, which is very important for system control while the direct model is used for system simulation; moreover, the closed-form dynamic equations can also be obtained via Newton-Euler method for the chain mechanisms. This method was utilized by Do and Yang [18] for the inverse dynamic analysis of Stewart platform, but the friction was left out of account and the pods were assumed as symmetrical and thin in the analysis. Dasgupta and Mruthyunjaya [19] followed a similar analysis for the inverse dynamics of Stewart platform, with the frictional forces occurring in the joints; meanwhile the mass of inertia of the pods were taken into consideration in their study. In another research the closed-form dynamic equations of the generally configured Stewart platform was developed by Dasgupta and Mruthyun-

---

jaya [20] through the Newton-Euler approach. In the last two references mentioned, the rotational degree of freedom of the pods around the axial direction is neglected to simplify the formulation. Furthermore, the moment of the universal joint is assumed in the direction of its pod and the theorem of parallel axes is not considered in obtaining inertia tensors of the different parts of the manipulator. Harib and Srinivasan [21] conducted the Newton-Euler method, and considered the effects of the different configuration of the joints on the angular velocities and accelerations of the pods. The kinematic model of the universal joint is considered in the kinematic analysis of their study, but similar simplifying approximations are used for deriving the inverse dynamic equations of the manipulator. Fu and Yao [22] compared the techniques used by Dasgupta and Mruthyunjaya in [19] with the Lagrange method, and made some suggestions as comments on them. Vakil et al. [23] also proposed some corrections as comments on two researches of Dasgupta and Mruthyunjaya [19, 20]. Mahmoodi et al. [24] used Newton-Euler method for the inverse dynamics of Stewart Platform, and utilized body coordinate frames for both platform and pods instead of inertial ones; they also considered the gyroscopic effects of the rotary parts within the pods for the sake of the faster rate of convergence. Pedrammehr et al. [25] improved the inverse dynamics of the general Stewart platform and presented the intact relations for the kinematics and dynamics of the mechanism.

This article presents an improved solution to the inverse kinematic and dynamic analyses of Stewart platform using Newton-Euler formulation with increasing the accuracy of modelling. The formulation incorporates all the gravity, inertia, coriolis, centripetal and external forces, and the intact angular velocity and acceleration for the pods; furthermore, viscose friction at the joints is also considered. Due to the accurate solution of the kinematic and dynamic problem of the manipulator, the kinematic model of the universal joint is introduced and the rotational degree of freedom of the pods around the axial direction is considered in deriving the kinematic and dynamic equations of the manipulator. This, however, adds to the complexity of the problem. The intact relations for the inertia tensors of different parts of the manipulator and the justifiable direction of the reaction moment on the pods are taken into account in order to derive the improved formulation. The newly-derived dynamic equations are completely different in comparison with the previously-introduced ones. In this study, in order to compare the results of the improved formulation with the simplified ones, the formulation has been implemented in a program written in MATLAB for kinematics and dynamics of the manipulator. The results of simulation are illustrated for the two improved and simplified models and their differences.

2. Stewart platform description

The mechanism under investigation consists of a moving platform, a stationary platform and six extensible pods (Fig. 1).
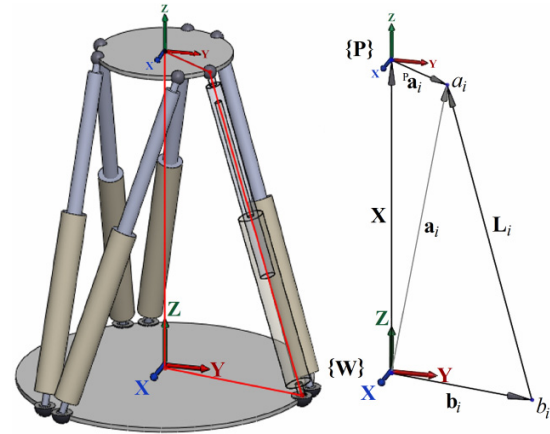
Fig. 1. Stewart platform and the vectorial representation of the ith pod.

Each pod connects to the platform at its connection point a_i through a spherical joint, and to the base at its connection point b_i through universal joint (i=1 to 6 for six pods). Each pod consists of two parts: the upper part and the lower part, which connect to each other through prismatic joint. Therefore, it is referred to as the 6-UPS Stewart platform. This familiar manipulator is actuated by motors located on the prismatic joints. The location and orientation of the moving platform frame {P}, is specified according to the base frame {W}; these frames are shown in Fig. 1.

3. Inverse kinematics

Inverse Kinematic problem of the platform involves determination of the linear position, velocity and acceleration of six pods through considering a specified position, velocity and acceleration of the moving platform centre.

The length vector of the ith pod can be obtained as:

$$\mathbf{L}_i = \mathbf{a}_i - \mathbf{b}_i \qquad (1)$$

where $\mathbf{a}_i$ and $\mathbf{b}_i$ are the position vectors of the ith platform and base connection points with the reference in base frame, respectively. $\mathbf{a}_i$ Can be obtained as:

$$\mathbf{a}_i = \mathbf{X} + \mathbf{q}_i \qquad (2)$$

and

$$\mathbf{q}_i = \mathbf{R}\,^P\mathbf{a}_i \qquad (3)$$

in which $\mathbf{X}$ is the position vector of the geometrical centre of the moving platform. $^P\mathbf{a}_i$ and $\mathbf{q}_i$ are the position vectors of the ith platform connection point in the moving frame and base frame, respectively. $\mathbf{R}$ is the rotation 3×3 matrix, representing the rotation of frame {P} related to frame {W}. Details for $\mathbf{R}$ are given in the Appendix 1.

Once $\mathbf{L}_i$ is determined, the length of the ith pod can be expressed as:

$$l_i = \|\mathbf{L}_i\| . \tag{4}$$

The unit vector along the direction of the ith pod can be obtained from:

$$\mathbf{n}_i = \mathbf{L}_i / l_i . \tag{5}$$

According to Eq. (5), the length vector of the ith pod can be expressed as:

$$\mathbf{L}_i = l_i \mathbf{n}_i . \tag{6}$$

By substituting Eq. (2) into Eq. (1), and equaling the resulting equation with Eq. (6) we can write:

$$l_i \mathbf{n}_i = \mathbf{X} + \mathbf{q}_i - \mathbf{b}_i . \tag{7}$$

Taking the derivative with respect to time on both sides of Eq. (7), and then by taking the dot product of the two sides of resulting equation with $\mathbf{n}_i$, The linear velocity of the ith pod $\dot{l}_i$ can be obtained as:

$$\dot{l}_i = \dot{\mathbf{X}} \cdot \mathbf{n}_i + \boldsymbol{\omega} \cdot (\mathbf{q}_i \times \mathbf{n}_i) \tag{8}$$

where $\dot{\mathbf{X}}$ and $\boldsymbol{\omega}$ are respectively the linear and angular velocity of the moving platform centre in the base frame.

The extensional acceleration of the ith pod $\ddot{l}_i$ can be obtained by taking the derivative with respect to time on both sides of Eq. (8), which yields:

$$\ddot{l}_i = \ddot{\mathbf{X}} \cdot \mathbf{n}_i + \boldsymbol{\alpha} \cdot (\mathbf{q}_i \times \mathbf{n}_i) + \dot{\mathbf{X}} \cdot (\boldsymbol{\omega}_{li} \times \mathbf{n}_i)$$
$$+ \boldsymbol{\omega} \cdot [(\boldsymbol{\omega} \times \mathbf{q}_i) \times \mathbf{n}_i + \mathbf{q}_i \times (\boldsymbol{\omega}_{li} \times \mathbf{n}_i)] \tag{9}$$

where $\ddot{\mathbf{X}}$ and $\boldsymbol{\alpha}$ are respectively the linear and angular acceleration of the moving platform centre in the base frame and $\boldsymbol{\omega}_{li}$ is the angular velocity of the ith pod.

4. Kinematics of the platform connection points

For a given motion of the moving platform, the motions of the six connection points of the pods to the platform can be simply determined.

The velocity of the ith platform connection point $\dot{\mathbf{L}}_i$ can be obtained by taking the derivative with respect to time on both sides of Eq. (6), which yields:

$$\dot{\mathbf{L}}_i = \boldsymbol{\omega}_{li} \times l_i \mathbf{n}_i + \dot{l}_i \mathbf{n}_i . \tag{10}$$

The acceleration of the ith platform connection point is also the time derivative of $\dot{\mathbf{L}}_i$, and can be expressed as:

$$\ddot{\mathbf{L}}_i = \boldsymbol{\alpha}_{li} \times l_i \mathbf{n}_i + \boldsymbol{\omega}_{li} \times (\boldsymbol{\omega}_{li} \times l_i \mathbf{n}_i) + 2\boldsymbol{\omega}_{li} \times \dot{l}_i \mathbf{n}_i + \ddot{l}_i \mathbf{n}_i \tag{11}$$

where $\boldsymbol{\alpha}_{li}$ is the angular acceleration of the ith pod.
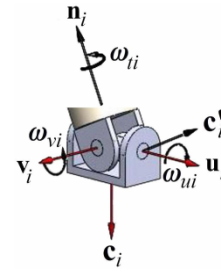
Fig. 2. Kinematic model of the universal joint.

5. Angular velocities and accelerations of the pods

Our knowledge of $\dot{l}_i$ and $\ddot{l}_i$ shows that we still cannot solve Eq. (10) for $\boldsymbol{\omega}_{li}$ and Eq. (11) for $\boldsymbol{\alpha}_{li}$, since 3×3 systems of the linear equations that result from the expanding Eqs. (10) and (11) are not full rank.

In the dynamic equations of previously-introduced models, the relations $\boldsymbol{\omega}_{li} \cdot \mathbf{n}_i = 0$ and $\boldsymbol{\alpha}_{li} \cdot \mathbf{n}_i = 0$ are utilized to facilitate the complexity of the formulation. These are simplifying approximations and may be true when there is no rotation around the axial direction. On the other hand, the rotation terms of the pods become even more significant in systems with electrical motion generators [24]; these terms are included for the inertia effects cannot be negligible in the machine tool applications also [15]. Therefore, an exact solution can be obtained by considering the rotational degree of freedom of the pods around the axial direction. in order to determine $\boldsymbol{\omega}_{li}$ and $\boldsymbol{\alpha}_{li}$, we need to use the kinematic model of the universal joint which is described in Fig. 2.

The unit vectors $\mathbf{u}_i$, $\mathbf{v}_i$ and $\mathbf{c}_i$ indicate the kinematic model of the universal joint, and the unit vectors $\mathbf{n}_i$, $\mathbf{v}_i$ and $\mathbf{c}'_i$ indicate the fixed pod frame. The unit vector $\mathbf{u}_i$ along the fixed axis of the universal joint can be obtained from the geometry of the mechanism. The unit vector $\mathbf{v}_i$ along the other revolute joint axis of the universal joint rotates in a plane normal to $\mathbf{u}_i$, and it is also normal to $\mathbf{n}_i$. The unit vector $\mathbf{c}_i$ is normal to the two axes of rotation of the universal joint and the unit vector $\mathbf{c}'_i$ is normal to $\mathbf{n}_i$ and $\mathbf{v}_i$.

As shown in Fig. 2, $\boldsymbol{\omega}_{li}$ can be resolved into two components along the two axes $\mathbf{u}_i$ and $\mathbf{v}_i$ of the universal joint, and can be defined as:

$$\boldsymbol{\omega}_{li} = \omega_{ui} \mathbf{u}_i + \omega_{vi} \mathbf{v}_i \tag{12}$$

where ω_{ui} and ω_{vi} are respectively the magnitudes of the components of $\boldsymbol{\omega}_{li}$ along the revolute joint axes $\mathbf{u}_i$ and $\mathbf{v}_i$, and can be obtained by substituting Eq. (12) into Eq. (10), and taking the dot product of the two sides of the resulting equation with $\mathbf{v}_i$ to solve for ω_{ui} and with $\mathbf{u}_i$ to solve for ω_{vi}, which yields:

$$\omega_{ui} = -(\dot{\mathbf{L}}_i - \dot{l}_i \mathbf{n}_i) \cdot \mathbf{v}_i / l_i \mathbf{n}_i \cdot \mathbf{c}_i \tag{13}$$

$$\omega_{vi} = (\dot{\mathbf{L}}_i - \dot{l}_i \mathbf{n}_i) \cdot \mathbf{u}_i / l_i \mathbf{n}_i \cdot \mathbf{c}_i . \tag{14}$$

On the other hand, $\boldsymbol{\omega}_{li}$ can be assumed as the combination of two components: a component along the direction of pod and the other along the direction perpendicular to the pod direction; therefore, it can be written as:

$$\boldsymbol{\omega}_{li} = \boldsymbol{\omega}_{ni} + \omega_{ti}\mathbf{n}_i \qquad (15)$$

in which $\boldsymbol{\omega}_{ni}$ is the component of $\boldsymbol{\omega}_{li}$ along the direction perpendicular to the direction of the pod, and ω_{ti} is the magnitude of the component of $\boldsymbol{\omega}_{li}$ along the direction of the pod.

$\boldsymbol{\omega}_{ni}$ can be obtained by substituting Eq. (15) into Eq. (10), and taking the cross product of the two sides of the resulting equation with $\mathbf{n}_i$, which yields:

$$\boldsymbol{\omega}_{ni} = (\mathbf{n}_i \times \dot{\mathbf{L}}_i)/l_i . \qquad (16)$$

According to Eq. (12), $\boldsymbol{\omega}_{li}$ is the combination of components along the axes $\mathbf{u}_i$ and $\mathbf{v}_i$; thus, $\boldsymbol{\omega}_{li}$ is in the cross plane and $\mathbf{c}_i$ indicates the normal vector to the plane resulting from vectors $\mathbf{u}_i$ and $\mathbf{v}_i$ (i.e. $\boldsymbol{\omega}_{li} \cdot \mathbf{c}_i = 0$); Therefore, ω_{ti} can be obtained by taking the dot product of the two sides of Eq. (15) with $\mathbf{c}_i$, which yields:

$$\omega_{ti} = -\boldsymbol{\omega}_{ni} \cdot \mathbf{c}_i / \mathbf{n}_i \cdot \mathbf{c}_i . \qquad (17)$$

$\boldsymbol{\alpha}_{li}$ can be obtained by taking the derivative with respect to time on both sides of Eq. (12), which yields:

$$\boldsymbol{\alpha}_{li} = \alpha_{ui}\mathbf{u}_i + \alpha_{vi}\mathbf{v}_i + \omega_{ui}\omega_{vi}\mathbf{c}_i \qquad (18)$$

in which α_{ui} and α_{vi} are the time derivatives of the ω_{ui} and ω_{vi}, respectively; and can be obtained by substituting Eq. (18) into Eq. (11), and taking the dot product of the two sides of the resulting equation with $\mathbf{v}_i$ to solve for α_{ui} and with $\mathbf{u}_i$ to solve for α_{vi}, which yields:

$$\alpha_{ui} = -\ddot{\mathbf{L}}_i' \cdot \mathbf{v}_i / l_i\mathbf{n}_i \cdot \mathbf{c}_i \qquad (19)$$

$$\alpha_{vi} = \ddot{\mathbf{L}}_i' \cdot \mathbf{u}_i / l_i\mathbf{n}_i \cdot \mathbf{c}_i \qquad (20)$$

where

$$\ddot{\mathbf{L}}_i' = \ddot{\mathbf{L}}_i - \omega_{ui}\omega_{vi} \times l_i\mathbf{n}_i - \boldsymbol{\omega}_{li} \times (\boldsymbol{\omega}_{li} \times l_i\mathbf{n}_i) - 2\dot{l}_i\boldsymbol{\omega}_{li} \times \mathbf{n}_i - \ddot{l}_i\mathbf{n}_i . \qquad (21)$$

On the other hand, $\boldsymbol{\alpha}_{li}$ can be considered as the combination of two components: one along the direction of the pod and the other along the direction perpendicular to the axial direction; therefore, it can be written as:

$$\boldsymbol{\alpha}_{li} = \boldsymbol{\alpha}_{ni} + \alpha_{ti}\mathbf{n}_i \qquad (22)$$

where $\boldsymbol{\alpha}_{ni}$ is the component of $\boldsymbol{\alpha}_{li}$ along the direction perpendicular to the pod direction, and α_{ti} is the magnitude of the component of $\boldsymbol{\alpha}_{li}$ along the direction of the pod.

$\boldsymbol{\alpha}_{ni}$ can be obtained by substituting Eq. (22) into Eq. (11), and taking the cross product of the two sides of the resulting equation with $\mathbf{n}_i$, which yields:

$$\boldsymbol{\alpha}_{ni} = \{\mathbf{n}_i \times \ddot{\mathbf{L}}_i - \mathbf{n}_i \times [\boldsymbol{\omega}_{li} \times (\boldsymbol{\omega}_{li} \times l_i\mathbf{n}_i) + 2\boldsymbol{\omega}_{li} \times \dot{l}_i\mathbf{n}_i]\}/l_i . \qquad (23)$$

Equaling Eqs. (18) and (22), and taking the dot product on the two sides of the resulting equation with $\mathbf{u}_i$ gives:

$$\alpha_{ui} = (\boldsymbol{\alpha}_{ni} + \alpha_{ti}\mathbf{n}_i) \cdot \mathbf{u}_i . \qquad (24)$$

α_{ti} can be obtained by using the above procedure but replacing $\mathbf{u}_i$ with $\mathbf{n}_i$, and then substituting Eq. (24) into the resulting equation, which gives:

$$\alpha_{ti} = [(\boldsymbol{\alpha}_{ni} \cdot \mathbf{u}_i)(\mathbf{u}_i \cdot \mathbf{n}_i)/1 - (\mathbf{u}_i \cdot \mathbf{n}_i)^2] - \omega_{ui}\omega_{vi} . \qquad (25)$$

6. Acceleration of the mass centres of the different parts of each pod

Before proceeding to the dynamics of the mechanism, we first need to determine expressions for the acceleration of the mass centres of different parts of each pod. These expressions, along with expressions for the angular velocity and acceleration of pods, as well as, expressions of linear velocity and acceleration of pods are all needed for the subsequent development of the rigid body dynamic equations in this paper.

Each pod contains two parts: an upper part, which is attached to the spherical joint and includes all the components that translate axially in addition to the rotational motion of the pod, and a lower part which is attached to the universal joint and includes all the remaining components that only rotate.

Mass centre position vectors of the lower and upper parts of the ith pod with reference to the fixed pod frame, $\mathbf{L}_{di}$ and $\mathbf{L}_{ui}$, are expressed as:

$$\mathbf{L}_{di} = \mathbf{T}_i \mathbf{L}_{doi} \qquad (26)$$

$$\mathbf{L}_{ui} = \mathbf{L}_i + \mathbf{T}_i \mathbf{L}_{uoi} \qquad (27)$$

where $\mathbf{L}_{doi}$ and $\mathbf{L}_{uoi}$ are respectively mass centre position vectors of the lower and upper parts of the ith pod in local frame of reference; and $\mathbf{T}_i$ is the transformation matrix from the moving lower and upper local frames to fixed pod frame and defined as:

$$\mathbf{T}_i = [\,\mathbf{n}_i \quad \mathbf{v}_i \quad \mathbf{c}_i'\,] . \qquad (28)$$

The accelerations of the mass centres of the lower and upper parts of the ith pod, $\ddot{\mathbf{L}}_{di}$ and $\ddot{\mathbf{L}}_{ui}$, are respectively the second time derivatives of $\mathbf{L}_{di}$ and $\mathbf{L}_{ui}$, and can be expressed as follows:

$$\ddot{\mathbf{L}}_{di} = \boldsymbol{\alpha}_{li} \times \mathbf{L}_{di} + \boldsymbol{\omega}_{li} \times (\boldsymbol{\omega}_{li} \times \mathbf{L}_{di}) \qquad (29)$$

$$\ddot{\mathbf{L}}_{ui} = \boldsymbol{\alpha}_{li} \times \mathbf{L}_{ui} + \boldsymbol{\omega}_{li} \times (\boldsymbol{\omega}_{li} \times \mathbf{L}_{ui}) + 2\boldsymbol{\omega}_{li} \times \dot{l}_i\mathbf{n}_i + \ddot{l}_i\mathbf{n}_i . \qquad (30)$$
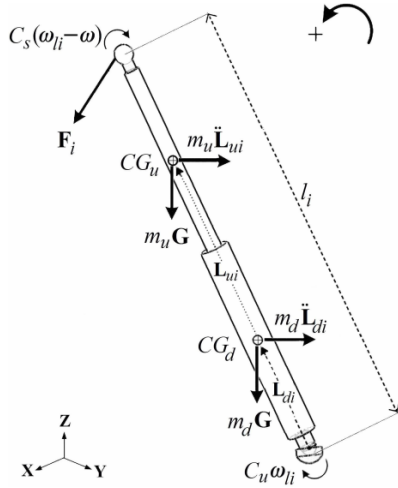
Fig. 3. Free body diagram of one pod.

7. Dynamics of pods

Fig. 3 shows the free body diagram of a single pod (represented as i^{th} one).

Considering a single pod consisting of two upper and lower parts, the equilibrium equation of moments about the centre point of the lower joint can be written as follows:

$$\mathbf{M}_i + l_i\mathbf{n}_i \times \mathbf{F}_i + (m_u\mathbf{L}_{ui} + m_d\mathbf{L}_{di}) \times \mathbf{G} - m_u\mathbf{L}_{ui} \times \ddot{\mathbf{L}}_{ui} - m_d\mathbf{L}_{di} \times \ddot{\mathbf{L}}_{di}$$
$$-(\mathbf{I}_{ui} + \mathbf{I}_{di})\boldsymbol{\alpha}_{li} - \boldsymbol{\omega}_{li} \times (\mathbf{I}_{ui} + \mathbf{I}_{di})\boldsymbol{\omega}_{li} - C_s(\boldsymbol{\omega}_{li} - \boldsymbol{\omega}) - C_u\boldsymbol{\omega}_{li} = 0 \tag{31}$$

where m_d and m_u are masses of the lower and upper parts of each pod, respectively; C_u and C_s are respectively the viscous friction coefficients in universal and spherical joints and $\mathbf{G}$ is the vector of gravity acceleration. $\mathbf{F}_i$ and $\mathbf{M}_i$ are the reaction force and moment of the ith pod in the base frame, respectively. $\mathbf{I}_{di}$ and $\mathbf{I}_{ui}$ are respectively the inertia tensors of the lower and upper parts of the ith pod.

The inertia tensor is a function of the location and orientation of the frame in which it is defined [26]. In the previously introduced models, the theorem of parallel axes has not been considered in the derivation of the inertia tensors of the different parts of the mechanism. Considering parallel axes theorem and using the vectors $\mathbf{L}_{di} = [l_{dx} \quad l_{dy} \quad l_{dz}]^T$ and $\mathbf{L}_{ui} = [l_{ux} \quad l_{uy} \quad l_{uz}]^T$, the inertia tensors of the upper and lower parts of the pod, $\mathbf{I}_{di}$ and $\mathbf{I}_{ui}$, can be expressed as:

$$\mathbf{I}_{di} = \mathbf{T}_i(\mathbf{I}_{doi} + m_d \begin{bmatrix} l_{dy}^2 + l_{dz}^2 & -l_{dx}l_{dy} & -l_{dx}l_{dz} \\ -l_{dx}l_{dy} & l_{dx}^2 + l_{dz}^2 & -l_{dy}l_{dz} \\ -l_{dx}l_{dz} & -l_{dy}l_{dz} & l_{dx}^2 + l_{dy}^2 \end{bmatrix})\mathbf{T}_i^T \tag{32}$$

$$\mathbf{I}_{ui} = \mathbf{T}_i(\mathbf{I}_{uoi} + m_u \begin{bmatrix} l_{uy}^2 + l_{uz}^2 & -l_{ux}l_{uy} & -l_{ux}l_{uz} \\ -l_{ux}l_{uy} & l_{ux}^2 + l_{uz}^2 & -l_{uy}l_{uz} \\ -l_{ux}l_{uz} & -l_{uy}l_{uz} & l_{ux}^2 + l_{uy}^2 \end{bmatrix})\mathbf{T}_i^T \tag{33}$$

in which $\mathbf{I}_{doi}$ and $\mathbf{I}_{uoi}$ are respectively the lower and upper

parts of the ith pod's inertia tensors at the coordinate frames attached to the centre of gravity of each part of the pod.

In the simplified models, the universal joint moment is assumed to be in the direction of its pod. Considering Fig. 2, there are no restriction moments at the $\mathbf{u}_i$ and $\mathbf{v}_i$ directions due to the revolute joints in these directions. Since the universal joint cannot impose any constraint moments in the $\mathbf{n}_i$, $\mathbf{u}_i$ and $\mathbf{v}_i$ directions, $\mathbf{M}_i$ is in the $\mathbf{c}_i$ direction and can be written as:

$$\mathbf{M}_i = m_i\mathbf{c}_i \tag{34}$$

where m_i is the magnitude of the $\mathbf{M}_i$.

Using Eq. (34), Eq. (31) can be rewritten compactly as:

$$m_i\mathbf{c}_i + l_i\mathbf{n}_i \times \mathbf{F}_i = \mathbf{N}_i \tag{35}$$

where

$$\mathbf{N}_i = -(m_u\mathbf{L}_{ui} + m_d\mathbf{L}_{di}) \times \mathbf{G} + m_u\mathbf{L}_{ui} \times \ddot{\mathbf{L}}_{ui} + m_d\mathbf{L}_{di} \times \ddot{\mathbf{L}}_{di}$$
$$+(\mathbf{I}_{ui} + \mathbf{I}_{di})\boldsymbol{\alpha}_{li} + \boldsymbol{\omega}_{li} \times (\mathbf{I}_{ui} + \mathbf{I}_{di})\boldsymbol{\omega}_{li} + C_s(\boldsymbol{\omega}_{li} - \boldsymbol{\omega}) + C_u\boldsymbol{\omega}_{li}. \tag{36}$$

By taking the dot product of both sides of Eq. (35) with $\mathbf{n}_i$, the magnitude of the reaction moment, can be determined as:

$$m_i = \mathbf{N}_i \cdot \mathbf{n}_i / \mathbf{c}_i \cdot \mathbf{n}_i. \tag{37}$$

$\mathbf{F}_i$ can be determined by taking the cross product of the two sides of Eq. (35) with $\mathbf{n}_i$, which yields:

$$\mathbf{F}_i = (\mathbf{n}_i \cdot \mathbf{F}_i)\mathbf{n}_i + [\mathbf{N}_i \times \mathbf{n}_i - m_i(\mathbf{c}_i \times \mathbf{n}_i)]/l_i. \tag{38}$$

In order to obtain the magnitude of the actuating force F_{acti}, Newton's equation in the pod direction for the upper part of the ith pod is separately considered as:

$$F_{acti} = -(\mathbf{n}_i \cdot \mathbf{F}_i) + m_u\mathbf{n}_i \cdot (\ddot{\mathbf{L}}_{ui} - \mathbf{G}) + C_p\dot{l}_i \tag{39}$$

in which C_p is the viscose friction coefficient at the prismatic joint; therefore, the term $C_p\dot{l}_i$ denotes frictional force occurring in the prismatic joint.

Eq. (37) and the expression for unknown $(\mathbf{n}_i \cdot \mathbf{F}_i)$ obtained from Eq. (39) can be substituted into Eq. (36), which gives:

$$\mathbf{F}_i = -F_{acti}\mathbf{n}_i + m_u[\mathbf{n}_i \cdot (\ddot{\mathbf{L}}_{ui} - \mathbf{G})]\,\mathbf{n}_i + C_p\dot{l}_i\mathbf{n}_i$$
$$+ [\mathbf{N}_i \times \mathbf{n}_i - (\mathbf{N}_i \cdot \mathbf{n}_i)\,(\mathbf{c}_i \times \mathbf{n}_i)/\mathbf{c}_i \cdot \mathbf{n}_i]/l_i. \tag{40}$$

Substituting Eq. (36) into Eq. (40), and substituting Eq. (30) into the resulting equation, and then using Eqs. (23), (22) and (9), which entail a number of algebraic vector operations, the compact expression for $\mathbf{F}_i$ can be obtained as:

$$\mathbf{F}_i = -F_{acti}\mathbf{n}_i + \mathbf{Q}_i(\ddot{\mathbf{X}} + \boldsymbol{\alpha} \times \mathbf{q}_i) + \mathbf{V}_i \tag{41}$$

where

$$\mathbf{Q}_i = m_u\ (\mathbf{n}_i\,\mathbf{n}_i^\mathbf{T}) + [\,m_u\,\tilde{\mathbf{n}}_i\,(\tilde{\mathbf{L}}_{ui})^2\tilde{\mathbf{n}}_i/l_i^2\,] + [\,m_d\,\tilde{\mathbf{n}}_i\,(\tilde{\mathbf{L}}_{di})^2\tilde{\mathbf{n}}_i/l_i^2\,]$$
$$-[\,\tilde{\mathbf{n}}_i(\mathbf{I}_{ui}+\mathbf{I}_{di})\tilde{\mathbf{n}}_i/l_i^2\,] + (\mathbf{c}_i\times\mathbf{n}_i/\mathbf{c}_i\cdot\mathbf{n}_i)\{\,[\,m_u\,\mathbf{n}_i^\mathbf{T}\,(\tilde{\mathbf{L}}_{ui})^2\tilde{\mathbf{n}}_i/l_i^2\,]$$
$$+[\,m_d\mathbf{n}_i^\mathbf{T}\,(\tilde{\mathbf{L}}_{di})^2\tilde{\mathbf{n}}_i/l_i^2\,] - \mathbf{n}_i^\mathbf{T}(\mathbf{I}_{ui}+\mathbf{I}_{di})\{\mathbf{n}_i\mathbf{u}_i^\mathbf{T}\mathbf{n}_i\mathbf{u}_i^\mathbf{T}\tilde{\mathbf{n}}_i/l_i^2[1-(\mathbf{u}_i\cdot\mathbf{n}_i)^2]\}\}$$

$$(42)$$

and

$$\mathbf{V}_i = m_u\{\mathbf{n}_i\cdot[\boldsymbol{\omega}_{li}\times(\boldsymbol{\omega}_{li}\times\mathbf{L}_{ui})]\}\ \mathbf{n}_i + m_u\{[\boldsymbol{\omega}\times(\boldsymbol{\omega}\times\mathbf{q}_i)]\cdot\mathbf{n}_i$$
$$-[\boldsymbol{\omega}_{li}\times(\boldsymbol{\omega}_{li}\times l_i\mathbf{n}_i)]\cdot\mathbf{n}_i\}\mathbf{n}_i - m_u\,(\mathbf{n}_i\cdot\mathbf{G})\,\mathbf{n}_i + C_p\,\dot{l}_i\,\mathbf{n}_i +$$
$$\{-[\,(m_u\mathbf{L}_{ui}+m_d\mathbf{L}_{di})\times\mathbf{G}]\times\mathbf{n}_i + m_u\,(\mathbf{n}_i\times\mathbf{S}_{ui}/l_i) + m_u\,\{\mathbf{L}_{ui}$$
$$\times[\boldsymbol{\omega}_{li}\times(\boldsymbol{\omega}_{li}\times\mathbf{L}_{ui})]\}\times\mathbf{n}_i + 2\,\dot{l}_i\,m_u\,[\mathbf{L}_{ui}\times(\boldsymbol{\omega}_{li}\times\mathbf{n}_i)]\times\mathbf{n}_i +$$
$$m_d\,(\mathbf{n}_i\times\mathbf{S}_{di}/l_i) + m_d\{\mathbf{L}_{di}\times[\boldsymbol{\omega}_{li}\times(\boldsymbol{\omega}_{li}\times\mathbf{L}_{ui})]\}\times\mathbf{n}_i - \{\mathbf{n}_i$$
$$\times[\,(\mathbf{I}_{ui}+\mathbf{I}_{di})\,\mathbf{S}_i\,]/l_i\} + [\boldsymbol{\omega}_{li}\times(\mathbf{I}_{ui}+\mathbf{I}_{di})\,\boldsymbol{\omega}_{li}]\times\mathbf{n}_i + C_u\,\boldsymbol{\omega}_{li}$$
$$\times\mathbf{n}_i + C_s(\boldsymbol{\omega}_{li}-\boldsymbol{\omega})\times\mathbf{n}_i\}/l_i - \{-[\,(m_u\,\mathbf{L}_{ui}+m_d\,\mathbf{L}_{di})\times\mathbf{G}]\cdot\mathbf{n}_i$$
$$-m_u(\mathbf{n}_i\cdot\mathbf{S}_{ui}/l_i) - m_d(\mathbf{n}_i\cdot\mathbf{S}_{di}/l_i) + \mathbf{n}_i\cdot(\mathbf{I}_{ui}+\mathbf{I}_{di})\{\{(\mathbf{u}_i\cdot\mathbf{S}_i)$$
$$(\mathbf{u}_i\cdot\mathbf{n}_i)\mathbf{n}_i/l_i[1-(\mathbf{u}_i\cdot\mathbf{n}_i)^2]\} - \omega_{ui}\omega_{vi}\,\mathbf{n}_i\} + [\boldsymbol{\omega}_{li}\times(\mathbf{I}_{ui}+\mathbf{I}_{di})$$
$$\boldsymbol{\omega}_{li}]\cdot\mathbf{n}_i + C_s\,(\boldsymbol{\omega}_{li}-\boldsymbol{\omega})\cdot\mathbf{n}_i + C_u\,\boldsymbol{\omega}_{li}\cdot\mathbf{n}_i\}[\mathbf{c}_i\times\mathbf{n}_i/l_i(\mathbf{c}_i\cdot\mathbf{n}_i)]\ .$$

$$(43)$$

The definitions of $\mathbf{S}_i$, $\mathbf{S}_{di}$ and $\mathbf{S}_{ui}$ are given in the Appendix 1.

In order to derive Eqs. (42) and (43), the following rules have been used in vector algebraic operations:

$$\mathbf{a}\times\mathbf{b} = \tilde{\mathbf{a}}\mathbf{b} \quad\text{and}\quad (\mathbf{a}\cdot\mathbf{b})\mathbf{c} = (\mathbf{c}\mathbf{a}^\mathbf{T})\mathbf{b} \tag{44}$$

where $\tilde{\mathbf{a}}$ is the skew symmetric matrix associated with the vector $\mathbf{a}$. The rules mentioned above refer to vectors which make reliable means as to translate vector algebraic operations into matrix multiplications.

In order to determine F_{acti}, we need to use the equations of motion for the platform which are derived in the next section.

8. Dynamics of the moving platform

The free body diagram of the platform is illustrated in Fig. 4. The vectors $\mathbf{F}_{ext}$ and $\mathbf{M}_{ext}$ are the external force and moment acting on the moving platform and described in the local frame of reference. These vectors can be expressed in the base frame of reference by the rotation transformation.

Considering Fig. 4, the force equilibrium equation can be obtained as:

$$m_p\ddot{\mathbf{X}}_g - m_p\mathbf{G} - \mathbf{R}\,\mathbf{F}_{ext} + \sum_{i=1}^{6}\mathbf{F}_i = 0 \tag{45}$$

where m_p is the mass of the platform and the payload. $\ddot{\mathbf{X}}_g$ is the linear acceleration of the mass centre of both the moving platform and the payload and can be obtained in terms of plat-
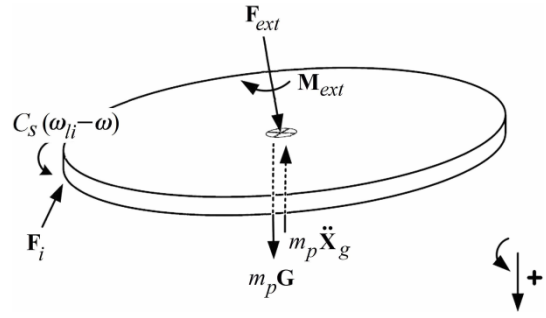
Fig. 4. Free body diagram of the moving platform.

form motion variables as:

$$\ddot{\mathbf{X}}_g = \ddot{\mathbf{X}} + \boldsymbol{\alpha}\times\mathbf{r} + \boldsymbol{\omega}\times(\boldsymbol{\omega}\times\mathbf{r}) \tag{46}$$

in which $\mathbf{r}$ is the mass centre position vector of the moving platform (including payload) in the base frame and can be expressed as:

$$\mathbf{r} = \mathbf{R}\,\mathbf{r}_o \tag{47}$$

where $\mathbf{r}_o$ denotes the mass centre position vector of the moving platform and the payload in the local frame of reference.

Substituting Eqs. (41) and (46) into Eq. (45) and using the rules (44), gives:

$$(m_p\mathbf{I}_3 + \sum_{i=1}^{6}\mathbf{Q}_i)\ddot{\mathbf{X}} - (m_p\tilde{\mathbf{r}} + \sum_{i=1}^{6}\mathbf{Q}_i\tilde{\mathbf{q}}_i)\boldsymbol{\alpha} + m_p[\boldsymbol{\omega}\times(\boldsymbol{\omega}\times\mathbf{r}) - \mathbf{G}]$$
$$+ \sum_{i=1}^{6}\mathbf{V}_i = \mathbf{R}\mathbf{F}_{ext} + \sum_{i=1}^{6}F_{acti}\mathbf{n}_i \tag{48}$$

where $\mathbf{I}_3$ denotes the 3×3 identity matrix.

The moment equilibrium equation about the geometrical centre of the platform can be written as:

$$m_p\mathbf{r}\times\ddot{\mathbf{X}}_g - m_p\mathbf{r}\times\mathbf{G} - \mathbf{R}\mathbf{M}_{ext} + \mathbf{I}_p\boldsymbol{\alpha} + \boldsymbol{\omega}\times\mathbf{I}_p\boldsymbol{\omega}$$
$$- \sum_{i=1}^{6}C_s(\boldsymbol{\omega}_{li}-\boldsymbol{\omega}) + \sum_{i=1}^{6}(\mathbf{q}_i\times\mathbf{F}_i) = 0 \tag{49}$$

where $\mathbf{I}_p$ is the inertia tensor of the platform and the payload in the base frame. Once the vector $\mathbf{r} = [r_x\ \ r_y\ \ r_z]^\mathbf{T}$ is determined, considering the theorem of parallel axes, the inertia tensor of the platform and the payload can be expressed as:

$$\mathbf{I}_p = \mathbf{R}(^\mathbf{P}\mathbf{I}_p + m_p\begin{bmatrix} r_y^2+r_z^2 & -r_xr_y & -r_xr_z \\ -r_xr_y & r_x^2+r_z^2 & -r_yr_z \\ -r_xr_z & -r_yr_z & r_x^2+r_y^2 \end{bmatrix})\mathbf{R}^\mathbf{T} \tag{50}$$

in which $^\mathbf{P}\mathbf{I}_p$ is the inertia tensor of the moving platform in the local frame.

By substituting Eqs. (41) and (46) into Eq. (49) and using the rules (44), Eq. (49) can be rewritten as follows:

$$(m_p\tilde{\mathbf{r}} + \sum_{i=1}^{6}\tilde{\mathbf{q}}_i\mathbf{Q}_i)\ddot{\mathbf{X}} + [\mathbf{I}_p - m_p(\tilde{\mathbf{r}})^2 - \sum_{i=1}^{6}\tilde{\mathbf{q}}_i\mathbf{Q}_i\tilde{\mathbf{q}}_i]\boldsymbol{\alpha}$$

$$+ m_p\mathbf{r}\times[\boldsymbol{\omega}\times(\boldsymbol{\omega}\times\mathbf{r}) - \mathbf{G}] + \sum_{i=1}^{6}(\mathbf{q}_i\times\mathbf{V}_i) + \boldsymbol{\omega}\times\mathbf{I}_p\boldsymbol{\omega} \qquad (51)$$

$$- \sum_{i=1}^{6}C_s(\boldsymbol{\omega}_{li} - \boldsymbol{\omega}) = \mathbf{RM}_{ext} + \sum_{i=1}^{6}(\mathbf{q}_i\times F_{acti}\mathbf{n}_i) \ .$$

9. Simulation study

In order to demonstrate the necessity of the improvement of the formulation, a simulation study is performed for a typical Stewart platform with physical specifications presented in Appendix 2. For this purpose, the formulation has been implemented in a program written in MATLAB for kinematics and dynamics of Stewart platform. Initial conditions taken for the simulations are given in Appendix 2.

If the rotational degree of freedom of the pods around axial direction is negligible, the complexity of the problem will be reduced. This, from a theoretical point, will lead to a low precision of the formulation. Therefore, knowledge on the contribution of the tangential components of the angular velocities and accelerations of the pods has applications for improvement of the accuracy of the formulation.

To examine the effect of the simplifications employed in the previous models (i.e. $\boldsymbol{\omega}_{li}\cdot\mathbf{n}_i = 0$ and $\boldsymbol{\alpha}_{li}\cdot\mathbf{n}_i = 0$) on angular velocities and accelerations, an X directional actuation is assumed for platform motion. To do so, a simple straight line path with a constant velocity profile is considered and the orientation of the platform is conserved during the simulation (Path 1, Appendix 2).

The angular velocities and accelerations of the six pods obtained by the current model, which includes the kinematic model of the universal joint and the rotational degree of freedom of the pods, are simulated and illustrated in Figs. 5 and 6, respectively. In order to compare these results with those of the simplified model, the simplified angular velocities and accelerations, perpendicular to the direction of the pod, and the difference between two given models are also illustrated in Figs. 5 and 6, respectively.

The results of both simplified and improved models indicate that the angular velocity in pods 1, 2 and 6 of Fig. 5 and the angular acceleration in pod 3 of Fig. 6 show great extent of consistency . Therefore, in this path, the angular velocities and accelerations of the pods are perpendicular to the direction of the pod and the differences in other pods present the contribution of the tangential components in the angular velocities and accelerations of those pods.

For the sake of comparing, it would be effective to make use of the same geometric and inertial properties for the test manipulator, as well as, the same parameters of the path as those used in Ref. [19]. Therefore, straight line path has been planned in the Cartesian space and a trapezoidal velocity pro-
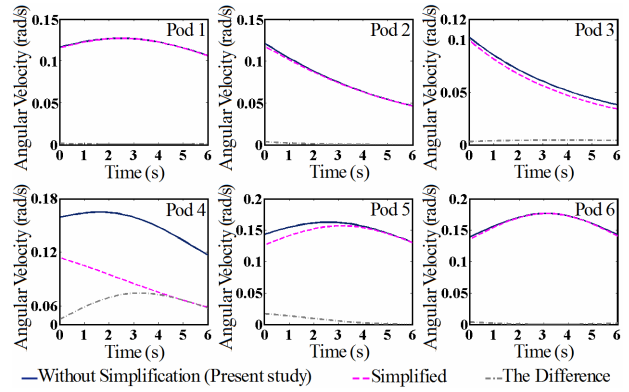
Fig. 5. Path 1; Angular velocities; without simplification (present study), simplified ($\boldsymbol{\omega}_{li}\cdot\mathbf{n}_i = 0$) and their difference.
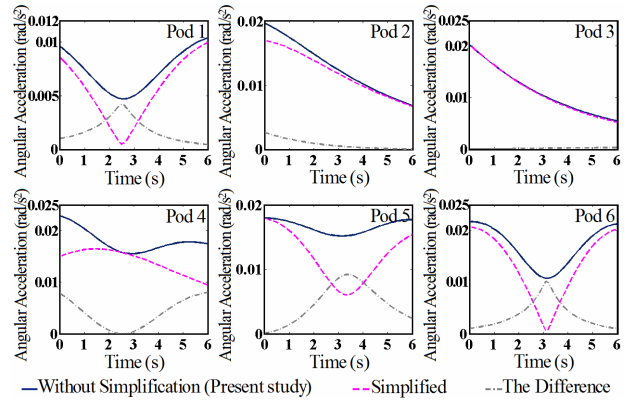
Fig. 6. Path 1; Angular accelerations; without simplification (present study), simplified ($\boldsymbol{\alpha}_{li}\cdot\mathbf{n}_i = 0$) and their difference.

file with constant acceleration at the beginning and constant deceleration at the end of the path is used for computer simulation. Moreover, similar expressions for the orientation of the platform are obtained (Path 2, Appendix 2).

The angular velocities and accelerations of the six pods obtained by kinematic analysis of the improved model are simulated and illustrated in Figs. 7 and 8, respectively; moreover, the simplified angular velocities and accelerations, which are perpendicular to the direction of the pod, and the difference between two mentioned models are compared in Figs. 7 and 8, respectively.

The comparative simulation has been done for the improved model and the reference model [19] for the dynamics of the manipulator in two different paths (i.e. Path 2 and Path 3 in Appendix 2). The results of the simulation for path 1 and path 2 are respectively illustrated in Figs. 9 and 10 as the plots of actuator forces required in the six pods to track the trajectory. The differences between the results of the models are also depicted.

The results shown in Figs. 9 and 10 indicate that both improved and simplified models exhibit similar trends of change, but difference in amplitudes. This, therefore, can be attributed to improvement effect. These improvements can be listed as follows:
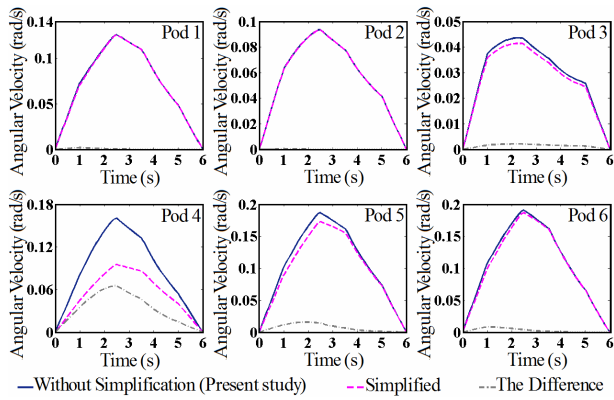
Fig. 7. Path 2; Angular velocities; without simplification (present study), simplified ($\boldsymbol{\omega}_{li} \cdot \mathbf{n}_i = 0$) and their difference.
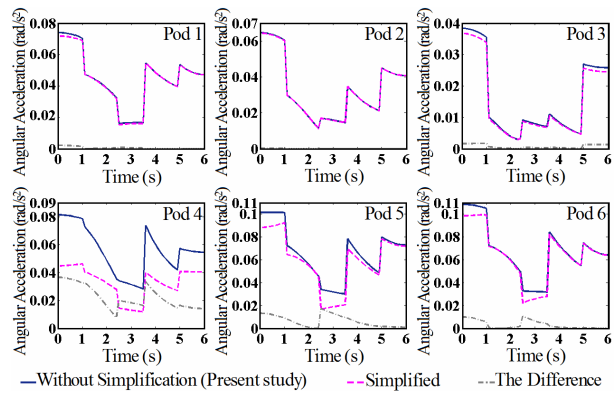
Fig. 8. Path 2; Angular accelerations; without simplification (present study), simplified ($\boldsymbol{\alpha}_{li} \cdot \mathbf{n}_i = 0$) and their difference.

Fig. 9. Path 2; Pod forces obtained by improved formulation (present study), simplified formulation and their difference.
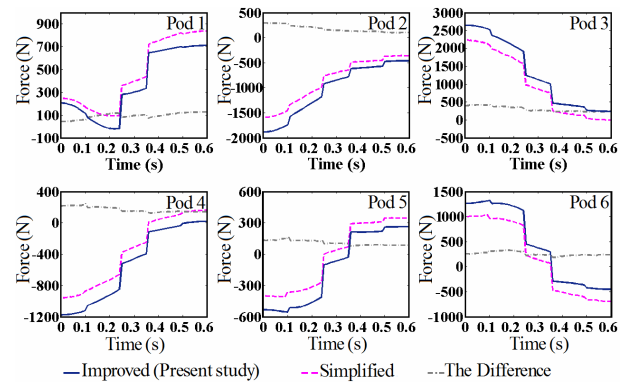
Fig. 10. Path 3; Pod forces obtained by improved formulation (present study), simplified formulation and their difference.

Taking to account the rotational degree of freedom of the pods around axial directions.

Considering the intact relations for angular velocities and acceleration of the pods through using kinematic model of the universal joint.

Considering the theorem of parallel axes and taking into account the intact relations for the inertia tensors of different parts of the pods as well as the intact relation for the inertia tensor of the moving platform.

Using the justifiable direction of the reaction moment on each pod and assuming that the universal joint cannot impose any constraint moments on the revolute joint axes and in the direction of pod.

Figs. 5-8 indicate that angular velocity or acceleration of a pod, given by both improved and simplified models will be identical if there is no rotation around the axial direction. But with the pod forces, the differences between simulation results, given by the improved model and the reference model [20], are quite obvious in Figs. 9 and 10. These significant differences indicate that improvements upon the system would be necessary shown in the current study for the formulation of the dynamic problem.

Convergence rate of the program is crucial in feedback linearization control [25]. The functions tic and toc are used in the code written in MATLAB to calculate elapsed CPU time for the improved algorithm. By using the specified processor (Intel®, Core™ 2Duo, 2.5 GHz, 4 GB RAM), the elapsed time for simulation of the mentioned paths through the improved model is 1.58 seconds.

10. Conclusions

In this paper a Newton-Euler method have been presented to solve the improved dynamic equations of the generally configured Stewart platform. The rotational degree of freedom of pods around related axial directions is considered in deriving the accurate relations of the angular velocities and accelerations of the pods. For this purpose, the kinematic model for the universal joint is introduced in the kinematic analysis of the manipulator. Considering the theorem of parallel axes, the intact relations for the inertia tensors of different parts of the manipulator are presented in this study. Moreover, in the dynamic relations of pods the justifiable direction of the reaction moment on each pod is introduced. It is easily concluded that the assumptions made on the previous researches have simplified and facilitate the formulation in comparison to what is presented here in this paper. The simulation outputs prove the new method significantly improved the dynamic equations

comparing to previous methods. The differences between the results of the improved formulation and those suggested in previously-introduced model are easily detected in the illustrations and provide the necessity of the improvements.

Appendix 1

The rotation matrix is obtained as:

$$\mathbf{R} = \begin{bmatrix} C\theta_z C\theta_y & -S\theta_z C\theta_x + C\theta_z S\theta_y S\theta_x & S\theta_z S\theta_x + C\theta_z S\theta_y C\theta_x \\ S\theta_z C\theta_y & C\theta_z C\theta_x + S\theta_z S\theta_y S\theta_x & -C\theta_z S\theta_x + S\theta_z S\theta_y C\theta_x \\ -S\theta_y & C\theta_y S\theta_x & C\theta_y C\theta_x \end{bmatrix}$$

where

$$C\theta_x = \cos(\theta_x) \quad \text{and} \quad S\theta_x = \sin(\theta_x)$$

in which θ_x, θ_y and θ_z are the Euler angles.

The terms $\mathbf{S}_i$, $\mathbf{S}_{di}$ and $\mathbf{S}_{ui}$ are defined as follows:

$$\mathbf{S}_i = \{\mathbf{n}_i \times [\boldsymbol{\omega} \times (\boldsymbol{\omega} \times \mathbf{q}_i) - \boldsymbol{\omega}_{li} \times (\boldsymbol{\omega}_{li} \times l_i \mathbf{n}_i) - 2\boldsymbol{\omega}_{li} \times \dot{l}_i \mathbf{n}_i]\}$$
$$\mathbf{S}_{di} = [\mathbf{L}_{di} \times (\mathbf{L}_{di} \times \mathbf{S}_i)]$$
$$\mathbf{S}_{ui} = [\mathbf{L}_{ui} \times (\mathbf{L}_{ui} \times \mathbf{S}_i)].$$

Appendix 2

The kinematic and dynamic specifications of the test manipulator are assumed as follows (all the quantities are given in SI units):

Connection points on the moving platform with reference to frame {**P**} :

$${}^{\mathrm{P}}\mathbf{a}_i = \begin{bmatrix} 0.3 & 0.3 & 0.0 & -0.2 & -0.15 & 0.15 \\ 0.0 & 0.2 & 0.3 & 0.1 & -0.20 & -0.15 \\ 0.1 & 0.0 & 0.0 & -0.1 & -0.05 & -0.05 \end{bmatrix}.$$

Connection points on the base platform with reference to frame {**W**} :

$$\mathbf{b}_i = \begin{bmatrix} 0.6 & 0.1 & -0.3 & -0.3 & 0.2 & 0.5 \\ 0.2 & 0.5 & 0.3 & -0.4 & -0.3 & -0.2 \\ 0.0 & 0.1 & 0.1 & 0.0 & -0.05 & 0.0 \end{bmatrix}.$$

Mass of the platform (including payload) and upper and lower parts of the pods:

$$m_p = 40.0$$
$$m_d = 3.0$$
$$m_u = 1.0.$$

Coefficients of the joints viscous friction:

$$C_u = 0.0001$$
$$C_p = 0.001$$
$$C_s = 0.0002.$$

Mass centres of the lower and upper parts of each pod in local frames:

$$\mathbf{L}_{doi} = \begin{bmatrix} 0.4 & 0.14 & -0.18 \end{bmatrix}^{\mathrm{T}}$$
$$\mathbf{L}_{uoi} = \begin{bmatrix} -0.6 & -0.08 & -0.08 \end{bmatrix}^{\mathrm{T}}.$$

Inertia tensors of the lower and upper parts of each pod in their local frames:

$$\mathbf{I}_{doi} = \begin{bmatrix} 0.01 & 0.005 & 0.007 \\ 0.005 & 0.002 & 0.003 \\ 0.007 & 0.003 & 0.001 \end{bmatrix}$$
$$\mathbf{I}_{uoi} = \begin{bmatrix} 0.005 & 0.002 & 0.002 \\ 0.002 & 0.002 & 0.001 \\ 0.002 & 0.001 & 0.003 \end{bmatrix}.$$

Mass centre of the moving platform and the payload in platform frame:

$$\mathbf{r}_o = \begin{bmatrix} 0.04 & 0.03 & -0.06 \end{bmatrix}^{\mathrm{T}}.$$

Inertia tensor of the moving platform and the payload in the platform frame:

$${}^{\mathrm{P}}\mathbf{I}_p = \begin{bmatrix} 0.05 & 0.003 & 0.004 \\ 0.003 & 0.04 & 0.003 \\ 0.004 & 0.003 & 0.10 \end{bmatrix}.$$

Initial conditions of the paths assumed for simulations are as follows:

Path 1 (X directional actuation):

The position vectors of the moving platform centre at the beginning and end of the simulation, $\mathbf{X}_0$ and $\mathbf{X}_t$ are assumed as follows:

$$\mathbf{X}_0 = \begin{bmatrix} 0.1 & 0.0 & 0.5 \end{bmatrix}^{\mathrm{T}}$$
$$\mathbf{X}_t = \begin{bmatrix} 0.6 & 0.0 & 0.5 \end{bmatrix}^{\mathrm{T}}.$$

The moving platform is disoriented and the orientation is kept unchanged during the simulation.

Total duration of simulation t, and the magnitudes of maximum linear velocity of the moving platform centre, $\dot{\mathbf{X}}$ is taken as follows:

$$t = 6.0$$
$$\dot{\mathbf{X}} = 0.08.$$

Path 2:

The position vectors of the moving platform centre at the beginning and end of the simulation, $\mathbf{X}_0$ and $\mathbf{X}_t$, and the orientations of the moving platform at the beginning and end of the simulation, $\boldsymbol{\theta}_0$ and $\boldsymbol{\theta}_t$, are assumed as follows:

$$\mathbf{X}_0 = \begin{bmatrix} 0.1 & 0.0 & 0.4 \end{bmatrix}^T$$
$$\mathbf{X}_t = \begin{bmatrix} 0.3 & 0.0 & 0.6 \end{bmatrix}^T$$
$$\boldsymbol{\theta}_0 = \begin{bmatrix} 0.0 & 0.0 & -0.2 \end{bmatrix}^T$$
$$\boldsymbol{\theta}_t = \begin{bmatrix} 0.0 & 0.0 & 0.2 \end{bmatrix}^T .$$

Total duration of simulation t, and the magnitudes of maximum linear and angular velocities of the moving platform centre, $\dot{\mathbf{X}}$ and ω, are taken as follows:

$$t = 6.0$$
$$\dot{\mathbf{X}} = 0.08$$
$$\omega = 0.08 .$$

Path 3:

Path 3 is as same as path 2, but with a higher speed and lower duration of the simulation. Therefore, the parameters $\mathbf{X}_0$, $\mathbf{X}_t$, $\boldsymbol{\theta}_0$ and $\boldsymbol{\theta}_t$ are kept unchanged, and the other parameters are assumed as follows:

$$t = 0.6$$
$$\dot{\mathbf{X}} = 0.8$$
$$\omega = 0.8 .$$

The external force $\mathbf{F}_{ext}$ and moment $\mathbf{M}_{ext}$ have been assumed as zero for the simulations.

References

[1] D. Stewart, A platform with six degrees of freedom, *Proc. Inst. Mech. Eng. Part C: J. Mech. Eng. Sci.,* 180 (15) (1965) 371-386.

[2] L.-W. Tsai, Solving the inverse dynamics of Stewart-Gough manipulator by the principle of virtual work, *J. Mech. Des.* 122 (1) (2000) 3-9.

[3] S. Staicu, X.-J. Liu and J. Wang, Inverse dynamics of the HALF parallel manipulator with revolute actuators, *Nonlinear Dyn.,* 50 (1-2) (2007) 1-12.

[4] Y. Zhao and F. Gao, Inverse dynamics of the 6-dof out-parallel manipulator by means of the principle of virtual work, *Robotica,* 27 (2) (2009) 259-268.

[5] M. H. Abedinnasab and G. R. Vossoughi, Analysis of a 6-DOF redundantly actuated 4-legged parallel mechanism, *Nonlinear Dyn.,* 58 (1-2) (2009) 611-622.

[6] M.-J. Liu, C.-X. Li and C.-N. Li, Dynamics analysis of the Gough-Stewart platform manipulator, *IEEE Trans. Rob. Automat.,* 16 (1) (2000) 94-98.

[7] W. You, M.-X. Kong, Z-J. Du and L.-N. Sun, High efficient inverse dynamic calculation approach for a haptic device with pantograph parallel platform, *Multibody Syst. Dyn.,* 21 (3) (2009) 233-247.

[8] A. M. Lopes and F. Almeida, The generalized momentum approach to the dynamic modeling of a 6-dof parallel manipulator, *Multibody Syst. Dyn.,* 21 (2) (2009) 123-146.

[9] A. M. Lopes, Dynamic modeling of a Stewart platform using the generalized momentum approach, *Commun. Nonlinear Sci. Numer. Simulat.,* 14 (8) (2009) 3389-3401.

[10] K. Miller, Optimal design and modeling of spatial parallel manipulators, *Int. J. Robot. Res.,* 23 (2) (2004) 127-140.

[11] J. Gallardo, J. Rico, A. Frisoli, D. Checcacci and M. Bergamasco, Dynamics of parallel manipulators by means of screw theory, *Mech. Mach. Theory,* 38 (11) (2003) 1113-1131.

[12] S. Staicu and D. Zhang, A novel dynamic modelling approach for parallel mechanisms analysis, *Robot. Comput. Integr. Manufact.,* 24 (1) (2008) 167-72.

[13] Z. Geng, L. S. Haynes, J. D. Lee and R. L. Carroll, On the dynamic model and kinematic analysis of a class of Stewart platforms, *Robot. Auton. Syst.,* 9 (4) (1992) 237-254.

[14] G. Lebret, K. Liu and F. L. Lewis, Dynamic analysis and control of a Stewart platform manipulator, *J. Robotic. Syst.,* 10 (5) (1993) 629-655.

[15] Y. Ting, Y.-S. Chen and H.-C. Jar, Modeling and control for a Gough-Stewart platform CNC machine, *J. Robotic. Syst.,* 21 (11) (2004) 609-623.

[16] W. Wang, H.-Y. Yang, J. Zou, X.-D. Ruan and X. Fu, Optimal design of Stewart platforms based on expanding the control bandwidth while considering the hydraulic system design, *J. Zhejiang Univ. Sci. A,* 10 (1) (2009) 22-30.

[17] H. B. Guo and H. R. Li, Dynamic analysis and simulation of a six degree of freedom Stewart platform manipulator, *Proc. Inst. Mech. Eng. Part C: J. Mech. Eng. Sci.,* 220 (C1) (2006) 61-72.

[18] W. Q. D. Do and D. C. H. Yang, Inverse dynamic analysis and simulation of a platform type of robot, *J. Robot. Syst.,* 5 (3) (1998) 209-227.

[19] B. Dasgupta and T. S. Mruthyunjaya, A Newton-Euler formulation for the inverse dynamics of Stewart platform manipulator, *Mech. Mach. Theory,* 33 (8) (1998) 1135-1152.

[20] B. Dasgupta and T. S. Mruthyunjaya, Closed-form dynamic equations of the general Stewart platform through Newton-Euler approach, *Mech. Mach. Theory*, 33 (7) (1998) 993-1012.

[21] K. Harib and K. Srinivasan, Kinematic and dynamic analysis of Stewart platform-based machine tool structures, *Robotica,* 21 (5) (2003) 541-554.

[22] S. Fu and Y. Yao, Comments on "A Newton-Euler formulation for the inverse dynamics of Stewart platform manipulator" by B. Dasgupta and T.S. Mruthyunjaya [Mech. Mach. Theory 33 (1998) 1135-1152], *Mech. Mach. Theory,* 42 (12) (2007) 1668-1671.

[23] M. Vakil, H. Pendar and H. Zohoor, Comments to the: "Closed-form dynamic equations of the general Stewart platform through the Newton-Euler approach" and "A Newton–

Euler formulation for the inverse dynamics of Stewart platform manipulator". *Mech. Mach. Theory,* 43 (10) (2008) 1349-1351.

[24] A. Mahmoodi, M. B. Menhaj and M. Sabzehparvar, An efficient method for solution of inverse dynamics of Stewart platform. *Aircraft Engineering and Aerospace Technology,* 81 (5) (2009) 398-406.

[25] S. Pedrammehr, M. Mahboubkhah and S. Pakzad, An improved solution to the inverse dynamics of the general Stewart platform, *IEEE International conference on mechatronics ICM 2011*, Istanbul, Turkey (2011).

[26] J. J. Craig, *Introduction to robotics: Mechanism and Control*. Second Ed., Addison-Wesley Publishing Co., Reading, MA (1989).

Mehran Mahboubkhah received his B.Sc. and M.Sc. in Mechanical Engineering from Amirkabir University of Technology and Sharif University of Technology, Tehran, Iran, in 1998 and 2000, respectively. He then received his Ph.D. in Mechanical Engineering from Tarbiat Modares University, Tehran, Iran, in 2008. Dr. Mahboubkhah is currently Assistant Professor in the Faculty of Mechanical Engineering in the University of Tabriz, Tabriz, Iran. His research interests include machine tools design, kinematic, dynamic, vibration and calibration of parallel kinematic machines and Metrology and Instrumentation.

Siamak Pedrammehr received his B.Sc. and M.Sc. in mechanical engineering from University of Tabriz, Tabriz, Iran, in 2008 and 2011, respectively. His research interests include kinematic and dynamic modeling and control of parallel mechanisms and machine tools, machining dynamics and modal analysis.

Navid Khani received the B.Sc. in mechanical engineering from Technical University of Tabriz, Tabriz, Iran, in 2008. He received his M.Sc. in mechanical engineering from University of Tehran, Tehran, Iran, in 2010. His research interests are numerical modeling and analysis of mechanical structures and manufacturing process.